

*Supporting Information for*

**Post-synthetic Modification of Ionic Liquids using  
Redox and Ligand Exchange Coordination Chemistry**

**Michael A. LeRoy<sup>a</sup>, Austin M. Mroz<sup>a</sup>, Jenna L. Mancuso<sup>a</sup>,**

**Aaron Miller<sup>a</sup>, Allison Van Cleve<sup>a</sup>, Casey Check<sup>b</sup>,**

**Hendrik Heinz<sup>c</sup>, Christopher H. Hendon<sup>a</sup>, Carl K. Brozek<sup>a\*</sup>**

*<sup>a</sup>Department of Chemistry and Biochemistry, Materials Science Institute,*

*University of Oregon, Eugene, OR 97405*

*<sup>b</sup>Center for Advanced Materials Characterization in Oregon*

*University of Oregon, Eugene, OR 97405*

*<sup>c</sup>Department of Chemical and Biological Engineering,*

*University of Colorado—Boulder, Boulder, CO 80309*

Email: cbrozek@uoregon.edu

**TABLE OF CONTENTS**

<b>Experimental Methods .....</b>	<b>S2</b>
<b>Supplementary Figures .....</b>	<b>S4</b>
<b>Figure S1.</b> Electronic absorption spectra of perhalometallate ILs.....	<b>S4</b>
<b>Figure S2.</b> Variable temperature viscosity of $[CoCl_4]^{2-}$ and $[CoBr_4]^{2-}$ ILs.....	<b>S5</b>
<b>Figure S3.</b> Cyclic voltammogram of $[HMIIm][VCl_4]$ IL .....	<b>S5</b>
<b>Figure S4.</b> $^{119}Sn$ NMR of $[HMIIm][SnCl_3]$ IL.....	<b>S6</b>
<b>Figure S5.</b> $^1H$ NMR of $[HMIIm]_2[SnCl_6]$ IL .....	<b>S6</b>
<b>Figure S6.</b> $^{119}Sn$ NMR of $[HMIIm]_2[SnCl_6]$ IL .....	<b>S7</b>
<b>Figure S7.</b> DSC of $[HMIIm]_2[SnCl_6]$ IL.....	<b>S7</b>
<b>Figure S8.</b> Variable temperature viscosity of $[CoCl_4]^{2-}$ ILs .....	<b>S8</b>
<b>Figure S9.</b> Electronic absorption spectra of $[NiCl_4]^{2-}$ ILs .....	<b>S8</b>
<b>Figure S10.</b> Variable temperature viscosity of $[VOCl_4]^{2-}$ ILs .....	<b>S9</b>
<b>Figure S11.</b> Variable temperature viscosity of $[FeCl_4]^-$ ILs .....	<b>S9</b>
<b>Figure S12.</b> Electrostatic potential maps for various imidazolium-based cations.....	<b>S10</b>
<b>Figure S13.</b> TD-DFT spectra of simulated $[OVCl_3]^-$ and $[OVCl_4]^{2-}$ anions .....	<b>S10</b>

<b>Figure S14.</b> Arrhenius plot of $[P_{6,6,6,14}]_2[CoCl_4]$ .....	S11
<b>Figure S15.</b> Arrhenius plot of $[P_{6,6,6,14}]_2[CoBr_4]$ .....	S11
<b>Figure S16.</b> Arrhenius plot of $[HMIm]_2[CoCl_4]$ .....	S12
<b>Figure S17.</b> Arrhenius plot of $[BM_2Im]_2[CoCl_4]$ .....	S12
<b>Figure S18.</b> Arrhenius plot of $[P_{6,6,6,14}][VCl_4]$ .....	S13
<b>Figure S19.</b> Arrhenius plot of $[P_{6,6,6,14}][FeCl_4]$ .....	S13
<b>Figure S20.</b> Arrhenius plot of $[HMIm][FeCl_4]$ .....	S14
<b>Figure S21.</b> Viscosity vs $E_a$ plot for various ILs .....	S14
<b>Figure S22.</b> Viscosity vs Free volume plot for various ILs .....	S15
<b>Figure S23.</b> Viscosity vs Molecular Volume ( $V_M$ ) plot for various ILs.....	S15
<b>Figure S24.</b> TGA of $[HMIm][VCl_4]$ and $[BM_2Im][VCl_4]$ .....	S16
<b>Figure S25.</b> XPS of $[P_{6,6,6,14}]_2[CoBr_4]$ after ligand exchange.....	S16
<b>Table S1.</b> Cartesian coordinates for optimized vanadium chloride structures.....	S16
<b>Table S2.</b> Viscoelastic and volumetric properties of selected ILs .....	S20
<b>References</b> .....	S20

## Experimental Methods

### Synthesis

#### Imidazolium derivatives

**[BMIm]<sub>2</sub>[CoCl<sub>4</sub>] (1).** In a 10-mL Schlenk flask 260 mg (2 mmol) CoCl<sub>2</sub> and 700 mg (4 mmol) 1-butyl-3-methylimidazolium (BMIm) chloride were combined under an inert atmosphere. The reaction mixture was then heated at 115°C for 2 hours with stirring. The resulting dark blue ionic liquid was stored under N<sub>2</sub>.

Compounds (2) [BMIm]<sub>2</sub>[NiCl<sub>4</sub>], a dark blue liquid, (3) [BMIm]<sub>2</sub>[CuCl<sub>4</sub>], a light orange liquid, and (4) [BMIm]<sub>2</sub>[MnCl<sub>4</sub>], a pale yellow liquid, were prepared in a similar fashion. Compounds (5) [BMIm][CrCl<sub>4</sub>], a dark purple liquid, and (6) [BMIm][FeCl<sub>4</sub>], an orange liquid, were similarly synthesized but by using a 1:1 mixture of the precursors.

**[HMIm]<sub>2</sub>[CoCl<sub>4</sub>] (7).** In a 10-mL Schlenk flask 260 mg (2 mmol) CoCl<sub>2</sub> and 810.88 mg (4 mmol) 1-n-hexyl-3-methylimidazolium (HMIm) chloride were combined under inert an atmosphere. The reaction mixture was then heated at 115°C for 2 hours with stirring. The resulting blue ionic liquid was stored under N<sub>2</sub>.

Compounds (8) [HMIm]<sub>2</sub>[NiCl<sub>4</sub>], a dark blue liquid, and (9) [HMIm]<sub>2</sub>[SnCl<sub>6</sub>], a light-yellow liquid, were prepared in a similar fashion. Compounds (10) [HMIm][SnCl<sub>3</sub>], a light-yellow liquid,

**(11)** [HMIIm][VCl<sub>4</sub>], a purple liquid, and **(12)** [HMIIm][FeCl<sub>4</sub>], an orange liquid, were also similarly synthesized but by using a 1:1 mixture of the precursors.

**[BM<sub>2</sub>Im]<sub>2</sub>[CoCl<sub>4</sub>] (13).** In a 10-mL Schlenk flask 260 mg (2 mmol) CoCl<sub>2</sub> and 754.7 mg (4 mmol) 1-butyl-2,3-dimethylimidazolium (BM<sub>2</sub>Im) chloride were combined under an inert atmosphere. The reaction mixture was then heated at 115°C for 2 hours with stirring. The resulting blue ionic liquid was stored under N<sub>2</sub>.

Compound **(14)** [BM<sub>2</sub>Im]<sub>2</sub>[NiCl<sub>4</sub>], a blue liquid, was prepared in a similar fashion, whereas for compound **(15)** [BM<sub>2</sub>Im][VCl<sub>4</sub>], a indigo liquid, a 1:1 mixture of the precursors was used.

### Phosphonium derivatives

**[P<sub>6,6,6,14</sub>]<sub>2</sub>[CoCl<sub>4</sub>] (16).** In a 10-mL Schlenk flask 260 mg (2 mmol) CoCl<sub>2</sub> and 2.07 g (4 mmol) trihexyltetradecylphosphonium (P<sub>6,6,6,14</sub>) chloride were combined under an inert atmosphere. The reaction mixture was then heated at 115°C for 2 hours with stirring. The resulting blue ionic liquid was stored under N<sub>2</sub>.

Compound **(17)** [P<sub>6,6,6,14</sub>]<sub>2</sub>[NiCl<sub>4</sub>], a blue liquid, was prepared in a similar fashion, whereas compounds **(18)** [P<sub>6,6,6,14</sub>][VCl<sub>4</sub>], a blue liquid, **(19)** [P<sub>6,6,6,14</sub>][VBr<sub>4</sub>], a green liquid, **(20)** [P<sub>6,6,6,14</sub>]<sub>2</sub>[CoBr<sub>4</sub>], a blue liquid, and **(21)** [P<sub>6,6,6,14</sub>][FeCl<sub>4</sub>], an orange liquid, were prepared by combining precursors in a 1:1 mixture.

### Ligand Exchange of Perchlorocobaltate to Perbromocobaltate ILs

Ligand exchange was performed by first chilling 0.2856 g (0.244 mmol) of **(16)** [P<sub>6,6,6,14</sub>]<sub>2</sub>[CoCl<sub>4</sub>] to 4 °C and 2 mL of 1-M HBr to –20 °C for 4 hours. The HBr solution was added dropwise to the ionic liquid causing a gradual color change from dark blue to light green. After addition was completed the solution was vigorously stirred by use of a vortexer. The mixture was left to settle, forming an aqueous layer and droplets of the ionic liquid. The aqueous layer was removed, and the resulting IL washed with DI water and then dried in an oven at 110°C to remove any residual water. After ligand exchange, the new mass of the IL was 0.1856g giving an overall yield of 65%.

### Oxidation of Vanadium ILs

Vanadium ILs **(11)** [HMIIm][VCl<sub>4</sub>], **(15)** [BM<sub>2</sub>Im][VCl<sub>4</sub>], and **(18)** [P<sub>6,6,6,14</sub>][VCl<sub>4</sub>] were oxidized by exposure to air and followed by heating at 150°C for two days. Solution-phase ILs in MeCN were oxidized by exposure to air.

### TD-DFT Calculations

The ORCA 4.0.1.2 software package<sup>1</sup> was used for simulating electronic absorption spectra. The all-electron def2-TZVPD basis sets Gaussian basis sets developed by the Ahlrichs group were employed in all calculations,<sup>2,3</sup> with the def2/J auxiliary basis.<sup>4</sup> Calculations were performed at the spin-unrestricted level using the M06-L functional.<sup>5</sup> Geometry optimizations began from crystallographically determined structures. In calculations that fixed individual V-Cl bond distances, all other atomic positions were optimized. Otherwise, all positions were optimized. All calculations were performed with and without the Control of the Conductor-like Polarizable Continuum Model (CPCM)<sup>6</sup> using ethanol to model the ionic liquid medium, as has been performed.<sup>7</sup>

## Packing Coefficient Calculations

Density functional theory (DFT) was used to perform geometry optimizations for the individual cations and anions of interest, as implemented in Gaussian09.<sup>8</sup> Optimizations were performed using a RMS force convergence of  $10^{-5}$  hartree, except for trihexyltetradecylphosphonium which required  $10^{-4}$  hartree convergence due to the shallow potential energy surface for the *n*-aliphatic carbon chains. The electronic wavefunction was obtained with the GGA functional M06L,<sup>5,9</sup> with a triple zeta basis set, including polarization and diffuse functions on all atoms.<sup>10</sup>

Packing coefficients were calculated using the formulation previously presented by Mecozzi *et al.*,<sup>11</sup> where the packing coefficient is taken as the ratio between the sum of the anion and cation molecular volumes ( $V_m$ ) and the occupied volume ( $V_o$ ).

$$\text{Packing Coefficient} = \frac{\sum V_m}{V_o}$$

The occupied volume is derived using the experimental concentration. The molecular volumes are calculated using a previously reported method,<sup>12,13</sup> using the electrostatic potential returned by DFT.

## Supplementary Figures:

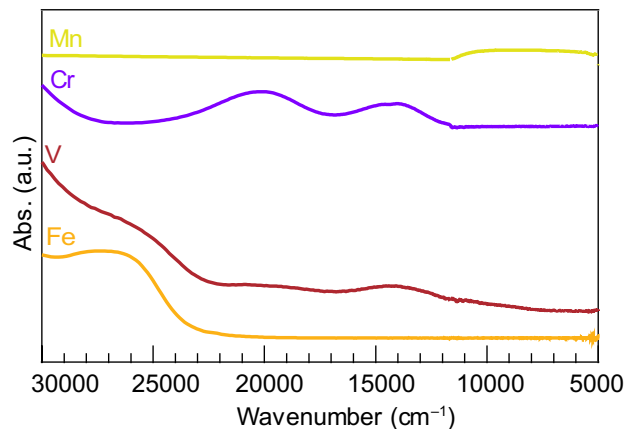


**Figure S1.** Electronic absorption spectra of neat ionic liquids 1-butyl-3-methylimidazolium (BMIm) perchlorometallate ions.  $[\text{BMIm}]_2[\text{MnCl}_4]$  in yellow,  $[\text{BMIm}]_2[\text{CrCl}_4]$  in purple, and  $[\text{BMIm}]_2[\text{VOCl}_4]$  in red, and  $[\text{BMIm}][\text{FeCl}_4]$  in orange.

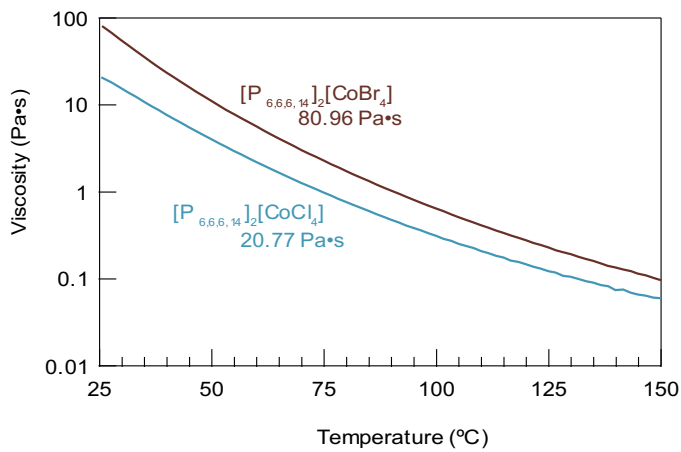


**Figure S2.** Temperature-dependent viscosities of  $[\text{CoCl}_4]^{2-}$  and  $[\text{CoBr}_4]^{2-}$  ionic liquids. Measurements collected between 25-150°C at 10 rad/s.

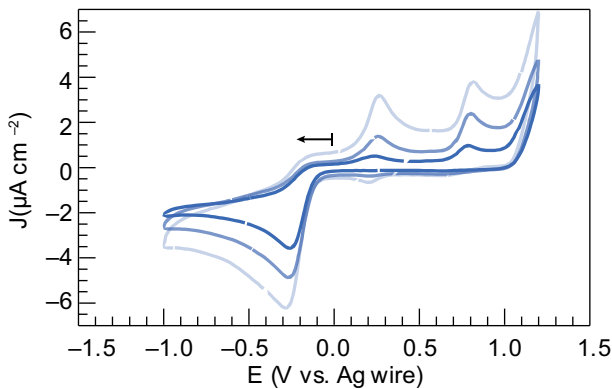


**Figure S3.** Cyclic voltammogram traces of mM  $[\text{P}_{6,6,6,14}][\text{VCl}_4]$  in acetonitrile. Scan rates were conducted at 25, 50 and 100 mV/s with a Pt wire W.E. and Ag wire C.E/R.E.

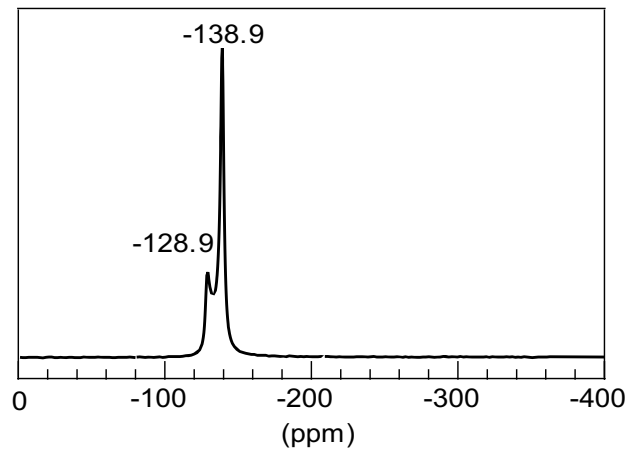


**Figure S4.**  $^{119}\text{Sn}$  NMR spectrum of neat  $\text{Sn}^{2+}$ -based  $[\text{HMIIm}][\text{SnCl}_3]$  ionic liquid.

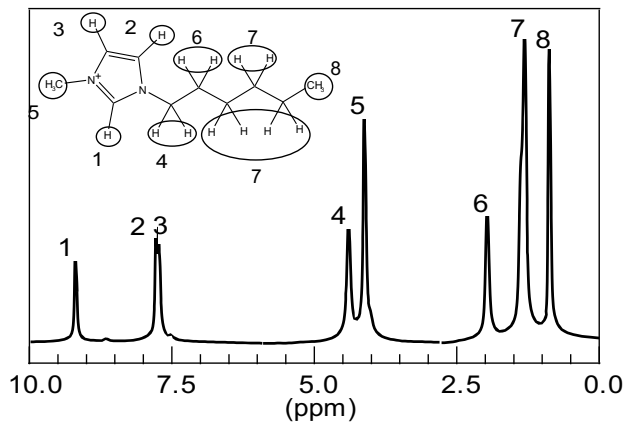


**Figure S5.**  $^1\text{H}$  NMR spectrum of neat  $\text{Sn}^{4+}$ -based  $[\text{HMIIm}]_2[\text{SnCl}_6]$  with assigned peaks.

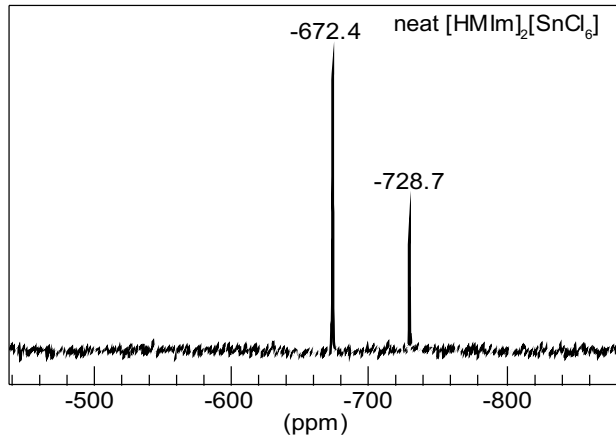


**Figure S6.**  $^{119}\text{Sn}$  NMR spectrum of  $\text{Sn}^{4+}$ -based  $[\text{HMIm}]_2[\text{SnCl}_6]$ .

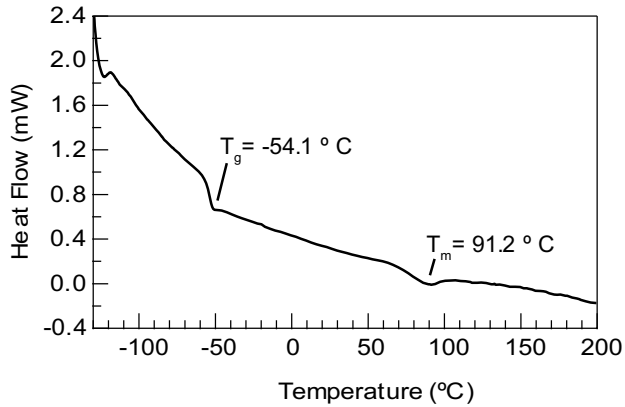


**Figure S7.** Differential scanning calorimetry scan (heating only, plotted with exothermic values as positive) of neat  $\text{Sn}^{4+}$ -based  $[\text{HMIm}]_2[\text{SnCl}_6]$  ionic liquid. Data shows a  $T_g$  at  $-54.1\text{ }^{\circ}\text{C}$  and  $T_m$  at  $91.2\text{ }^{\circ}\text{C}$ .

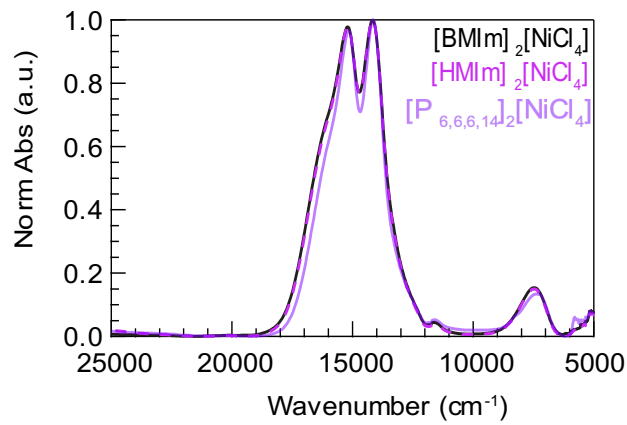
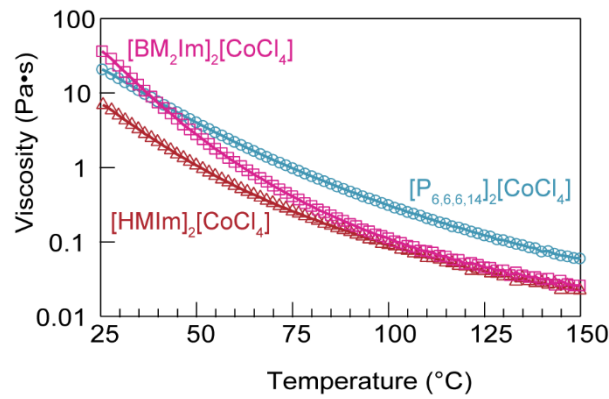


**Figure S9:** Absorption spectra of  $[\text{NiCl}_4]^{2-}$  ionic liquids with different imidazolium (HMIm and BMIm) and  $\text{P}_{6,6,6,14}$  cations.

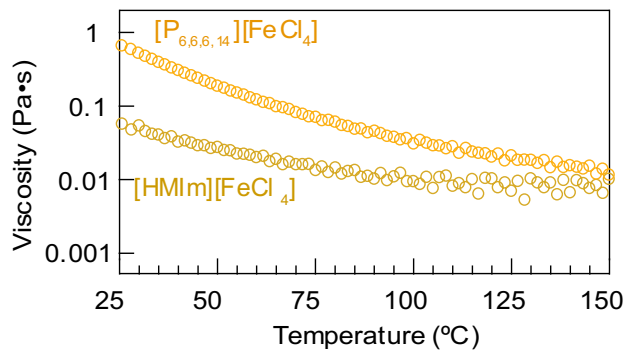
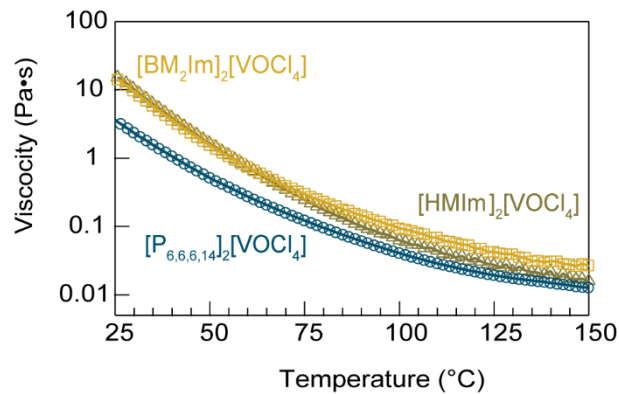


**Figure S11. Temperature dependent viscosities of  $[\text{FeCl}_4^-$ - ionic liquids containing HMIm and  $\text{P}_{6,6,6,14}$  cations.** Measurements collected between 25-150°C at 10 rad/s.

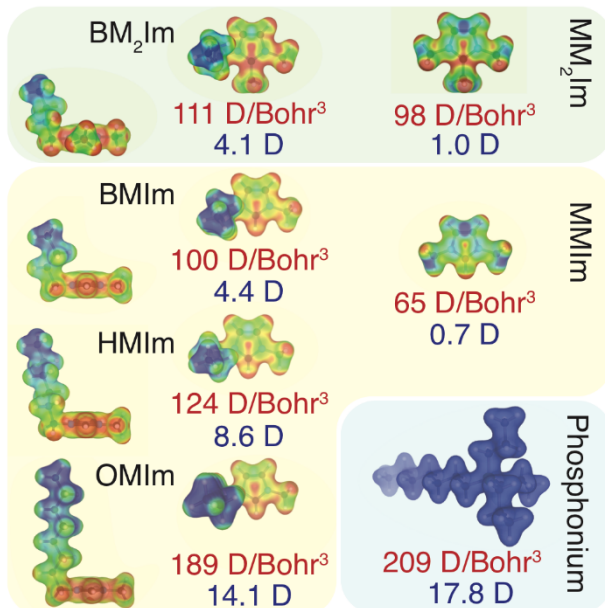


**Figure S12.** Electrostatic potential maps constructed for each cation explored herein and the methyl substituted imidazolium rings to illustrate the impact of electron-withdrawing alkyl substituents. Polarizabilities are presented in red text and dipole moments are shown in blue; within the maps, red corresponds to regions of relative positivity and blue, negativity. Increasing the length of the alkyl chain enhances the molecular polarizability and net dipole moment; it can also be seen that the proton in the 2 position increases in electrophilicity as the alkyl chain increases in length and that the 2,3-dimethyl variants show their greatest electrophilicity on the face of the ring, rather than in front.

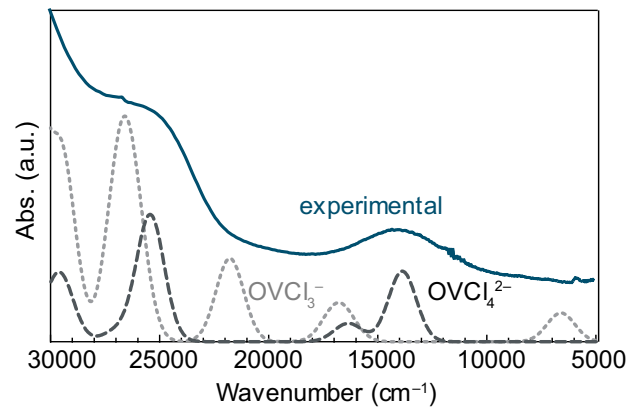


**Figure S13.** TD-DFT of simulated  $[\text{OVCl}_3]^-$  and  $[\text{OVCl}_4]^{2-}$  anions and experimental  $[\text{OVCl}_x]^{y-}$  spectra.

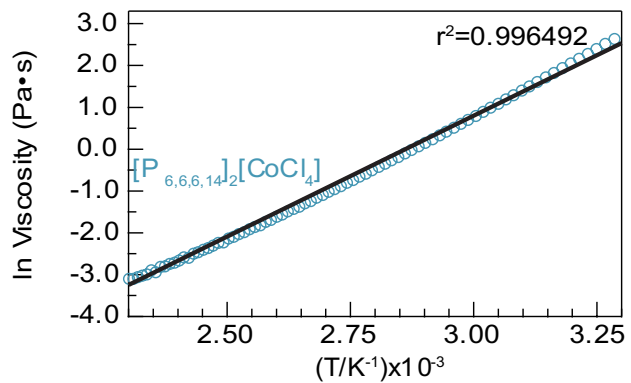


**Figure S14.** Arrhenius plot of  $[\text{P}_{6,6,6,14}]_2[\text{CoCl}_4]$  ( $r^2=0.996$ ).

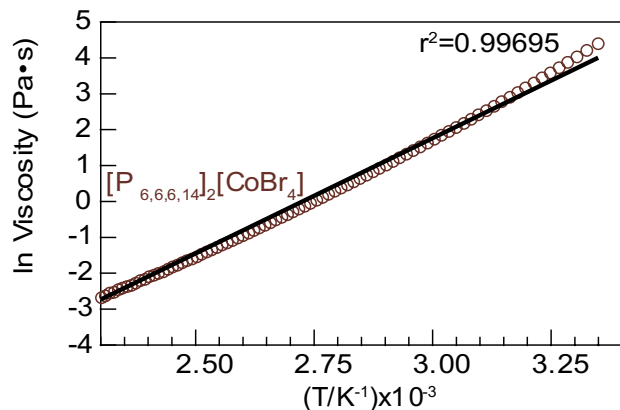


**Figure S15.** Arrhenius plot of  $[\text{P}_{6,6,6,14}]_2[\text{CoBr}_4]$  ( $r^2=0.996$ ).

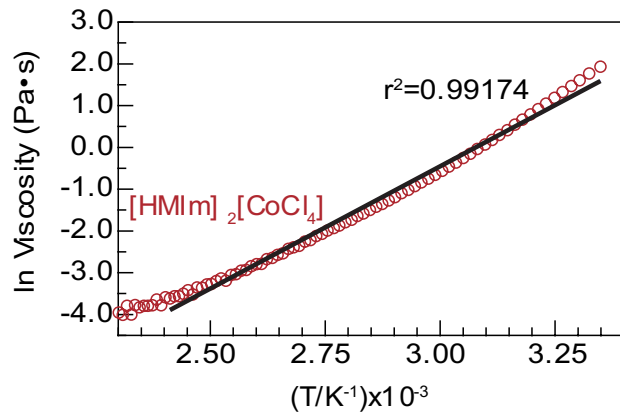


**Figure S16.** Arrhenius plot of  $[\text{HMIm}]_2[\text{CoCl}_4]$  ( $r^2=0.991$ ).

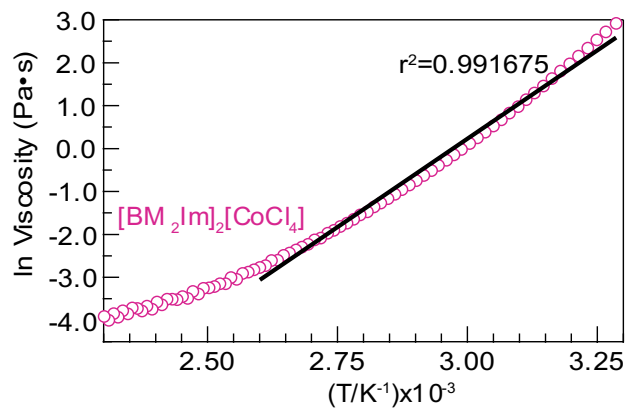


**Figure S17.** Arrhenius plot of  $[\text{BM}_2\text{Im}]_2[\text{CoCl}_4]$  ( $r^2=0.991$ ).

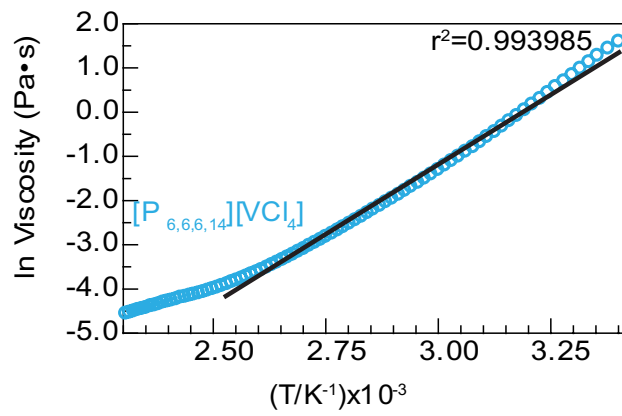


**Figure S18.** Arrhenius plot of  $[\text{P}_{6,6,6,14}][\text{VCl}_4]$  ( $r^2=0.993$ ).

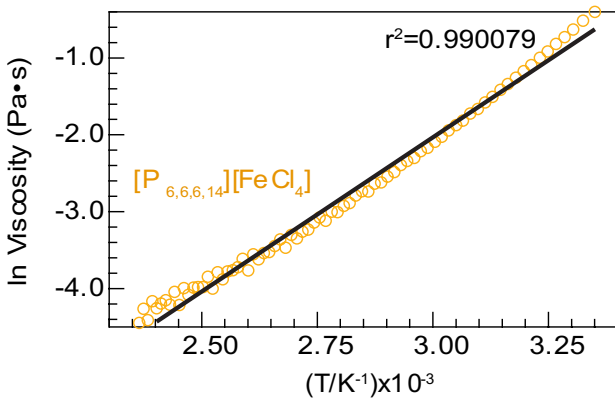


**Figure S19.** Arrhenius plot of  $[\text{P}_{6,6,6,14}][\text{FeCl}_4]$  ( $r^2=0.990$ ).

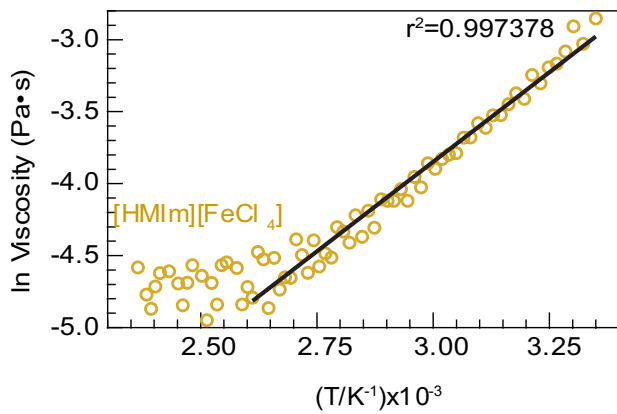


**Figure S20.** Arrhenius plot of  $[\text{HMIIm}][\text{FeCl}_4]$  ( $r^2=0.997$ ).

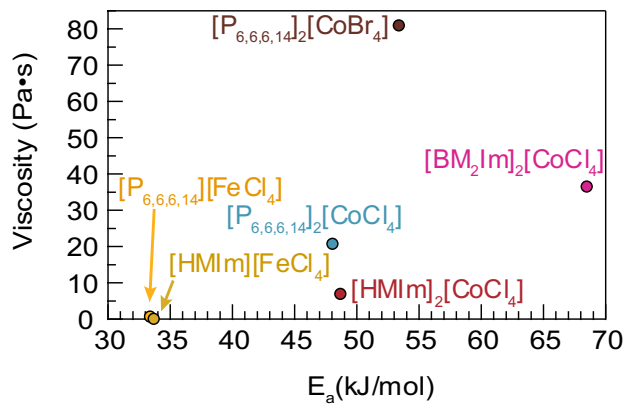


**Figure S21.** Viscosity vs  $E_a$  plot for various ILs reported here.

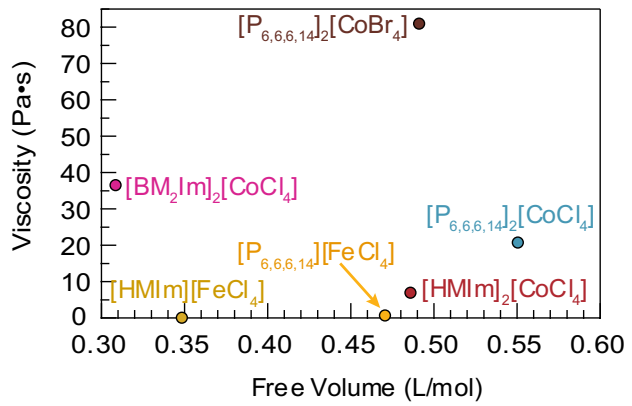


**Figure S22.** Viscosity vs Free volume plot for various ILs reported here.

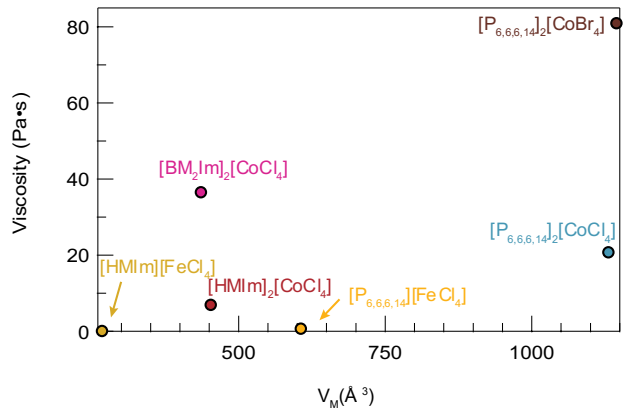


**Figure S23.** Viscosity vs Molecular volume plot for various ILs reported here.

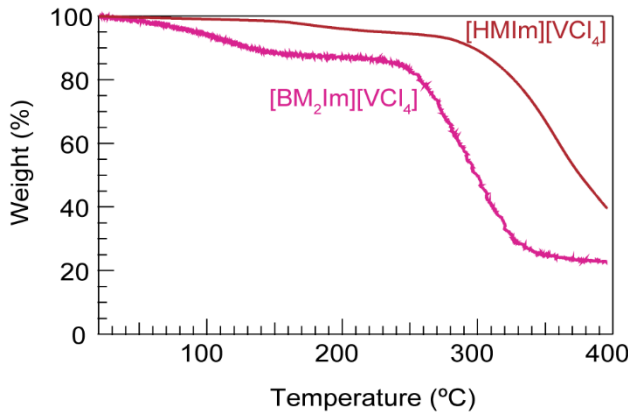


**Figure S24.** TGA of  $[HMIm][VCl_4]$  and  $[BM_2Im][VCl_4]$ .

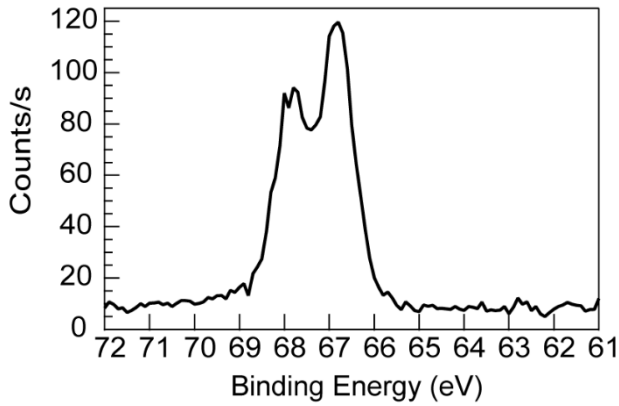


**Figure S25.** XPS of  $[P_{6,6,6,14}]_2[CoBr_4]$  after ligand exchange.

**Table S1.** Cartesian coordinates of the geometry-optimized  $VOCl_3^-$ ,  $VOCl_4^{2-}$ ,  $VCl_4^-$ ,  $VCl_6^{3-}$ , elongated V-Cl bond lengths, and dimer of  $VCl_6-VCl_3$ .

<u>VOCl<sub>3</sub></u>	<u>x</u>	<u>y</u>	<u>z</u>
V -6.54395396670483	-0.29232762795535	0.13184713553779	
Cl -4.30396504074253	-0.11286832297413	-0.10238102334569	
Cl -7.23366461651539	0.73328938622419	-1.79069871721589	
Cl -7.36885566219071	1.14310590690421	1.66904573937769	
O -7.16266071384653	-1.75805934219890	0.09218686564611	
<u>VOCl<sub>4</sub></u>	<u>x</u>	<u>y</u>	<u>z</u>
V -6.77774206956111	-0.32267787042807	-0.09851996408668	

Cl	-4.89066532554752	-0.95593506088053	1.24665349193267
Cl	-7.97581116882425	1.03030690377371	-1.68451249998524
Cl	-6.98694572187346	1.52266865101555	1.36158473423461
Cl	-5.48455985195872	-1.03532081020180	-1.94084159946864
O	-7.84948586223495	-1.43877181327886	0.27334583737328

<b>VCl<sub>4</sub></b>	<b>x</b>	<b>y</b>	<b>z</b>
V	-6.52030464311140	-0.05616575429708	-0.00320320170501
Cl	-4.27513726523367	-0.05913984233518	0.00671431729897
Cl	-7.27818443044818	0.82638884085433	-1.92263550953603
Cl	-7.26880567133938	1.16269435152964	1.72477074071618
Cl	-7.27066798986735	-2.16062759575171	0.19435365322590

<b>VCl<sub>6</sub></b>	<b>x</b>	<b>y</b>	<b>z</b>
V	-2.04827040285955	0.61559165990641	-0.00824454676758
Cl	-1.98505709364099	3.02199997188484	0.02765505294522
Cl	0.35125088724121	0.55196150754853	0.08208263580656
Cl	-2.11088756505193	-1.79076546605242	-0.04477317837910
Cl	-4.44827280465886	0.68004376450511	-0.09791734600515
Cl	-1.95109847850913	0.65116468755874	-2.46641657783130
Cl	-2.14766454252075	0.57938387464879	2.45056396023135

### **V-Cl Bond Length 230 ppm**

	<b>x</b>	<b>y</b>	<b>z</b>
V	-6.55789964977586	-0.00827422937702	-0.10046531344177
Cl	-4.31920704773071	0.00849748862575	-0.13142508719586
Cl	-7.32487137893691	0.90232275212788	-2.06834933155979
Cl	-7.32305357655084	1.23222344743809	1.59741948347180
Cl	-7.33057834700569	-2.10261945881471	0.05219024872562

### **V-Cl Bond Length 240 ppm**

	<b>x</b>	<b>y</b>	<b>z</b>
V	-6.52833381715816	-0.04657308607269	-0.01888738670304

Cl	-4.30324490329034	0.02246393583263	-0.16526161033795
Cl	-7.32676544947378	0.90718513159555	-2.07141075737732
Cl	-7.34613698007190	1.26993228123850	1.58578980987496
Cl	-7.35112885000581	-2.12085826259398	0.01913994454335

### **V-Cl Bond Length 245 ppm**

	<u>X</u>	<u>Y</u>	<u>Z</u>
V	-6.50757463363672	-0.06937119000275	0.03144229256899
Cl	-4.29299031998065	0.03231275962039	-0.18993753503235
Cl	-7.32532621015501	0.90366223683106	-2.06307156851530
Cl	-7.36339700696933	1.29071508995106	1.57469018479710
Cl	-7.36632182925828	-2.12516889639976	-0.00375337381843

### **V-Cl Bond Length 260 ppm**

	<u>X</u>	<u>Y</u>	<u>Z</u>
V	-6.47689731842737	-0.10708148137169	0.10769460935215
Cl	-4.28194073844320	0.04003428220193	-0.20558527361019
Cl	-7.34252320012089	0.93168046264819	-2.11304073317845
Cl	-7.37578764409360	1.30171298148820	1.57014499707245
Cl	-7.37846109891493	-2.13419624496663	-0.00984359963596

**V-Cl Bond Length 275 ppm**

	<u>X</u>	<u>Y</u>	<u>Z</u>
V	-6.45294780461319	-0.13549553655009	0.17189449288147
Cl	-4.27530519260705	0.04180868750040	-0.20411194058639
Cl	-7.36856901468163	0.95728298177204	-2.17969495142264
Cl	-7.37582047862366	1.30780206857354	1.57721415666044
Cl	-7.38296750947447	-2.13924820129588	-0.01593175753289

**V-Cl Bond Length 300 ppm**

	<u>X</u>	<u>Y</u>	<u>Z</u>
V	-6.41823680941886	-0.17415210552639	0.26611334320177
Cl	-4.26724913882586	0.03733815373071	-0.19321904489178
Cl	-7.41697229529935	1.00286368644475	-2.30627100776400
Cl	-7.37119566125940	1.30791372188408	1.59967371680589
Cl	-7.38195609519653	-2.14181345653315	-0.01692700735188

<u>Dimer</u>	<u>X</u>	<u>Y</u>	<u>Z</u>
V	3.22531	1.67175	17.34155
Cl	5.24275	1.91686	18.47855
Cl	3.80113	3.30304	15.73472
Cl	1.94261	3.04414	18.62522
Cl	1.52535	0.68638	16.04624
Cl	2.72630	-0.41616	18.86678
Cl	4.60530	-0.22168	15.97779
V	3.11477	-1.66213	16.96931
Cl	4.46817	-3.29354	17.69622
Cl	1.55936	-2.73064	15.77998

**Table S2. Viscoelastic and volumetric properties of selected ILs.**  $V_0$ : occupied volume.  $V_M$ : molecular volume.

Ionic Liquid	M.W. (g/mol)	Density (g/L)	Molarity (mol/L)	$V_0$ (L/mol)	$V_M$ (Å³)
[P <sub>6,6,6,14</sub> ] <sub>2</sub> [CoCl <sub>4</sub> ]	1168.46	1218	1.04	0.96	1130.50
[P <sub>6,6,6,14</sub> ] <sub>2</sub> [CoBr <sub>4</sub> ]	1346.26	1478	1.10	0.91	1144.28
[HMIm] <sub>2</sub> [CoCl <sub>4</sub> ]	535.28	714	1.33	0.75	452.59
[BM <sub>2</sub> Im] <sub>2</sub> [CoCl <sub>4</sub> ]	507.22	896	1.76	0.57	435.84
[P <sub>6,6,6,14</sub> ][FeCl <sub>4</sub> ]	790.26	1016	1.42	0.70	606.07
[HMIm][FeCl <sub>4</sub> ]	473.67	931	1.95	0.51	267.11

## References

- 1 F. Neese, *Wiley Interdiscip. Rev. Comput. Mol. Sci.*, 2018, **8**, 1–6.
- 2 F. Weigend and R. Ahlrichs, *Phys. Chem. Chem. Phys.*, 2005, **7**, 3297.
- 3 D. Rappoport and F. Furche, *J. Chem. Phys.*, 2010, **133**, 134105.
- 4 F. Weigend, *Phys. Chem. Chem. Phys.*, 2006, **8**, 1057.
- 5 Y. Zhao and D. G. Truhlar, *J. Chem. Phys.*, 2006, **125**, 194101.
- 6 V. Barone and M. Cossi, *J. Phys. Chem. A*, 1998, **102**, 1995–2001.
- 7 S. Chen and E. I. Izgorodina, *Phys. Chem. Chem. Phys.*, 2017, **19**, 17411.
- 8 Gaussian 09, Revision A.02, M. J. Frisch, G. W. Trucks, H. B. Schlegel, G. E. Scuseria, M. A. Robb, J. R. Cheeseman, G. Scalmani, V. Barone, G. A. Petersson, H. Nakatsuji, X. Li, M. Caricato, A. Marenich, J. Bloino, B. G. Janesko, R. Gomperts, B. Mennucci, H. P. Hratchian, J. V. Ortiz, A. F. Izmaylov, J. L. Sonnenberg, D. Williams-Young, F. Ding, F. Lipparini, F. Egidi, J. Goings, B. Peng, A. Petrone, T. Henderson, D. Ranasinghe, V. G. Zakrzewski, J. Gao, N. Rega, G. Zheng, W. Liang, M. Hada, M. Ehara, K. Toyota, R. Fukuda, J. Hasegawa, M. Ishida, T. Nakajima, Y. Honda, O. Kitao, H. Nakai, T. Vreven, K. Throssell, J. A. Montgomery, Jr., J. E. Peralta, F. Ogliaro, M. Bearpark, J. J. Heyd, E. Brothers, K. N. Kudin, V. N. Staroverov, T. Keith, R. Kobayashi, J. Normand, K. Raghavachari, A. Rendell, J. C. Burant, S. S. Iyengar, J. Tomasi, M. Cossi, J. M. Millam, M. Klene, C. Adamo, R. Cammi, J. W. Ochterski, R. L. Martin, K. Morokuma, O. Farkas, J. B. Foresman, and D. J. Fox, Gaussian, Inc., Wallingford CT, 2016.

- 9 Y. Zhao, D. G. Truhlar, Y. Zhao and · D G Truhlar, *Theor Chem Acc.*, 2008, **120**, 215–241.
- 10 T. Yanai, D. P. Tew and N. C. Handy, *Chem. Phys. Lett.*, 2004, **393**, 51–57.
- 11 S. Mecozzi and J. Rebek, Jr., *Chem. - A Eur. J.*, 1998, **4**, 1016–1022.
- 12 E. C. Sutton, C. E. Mcdevitt, J. Y. Prochnau, M. V Yglesias, A. M. Mroz, M. C. Yang, R. M. Cunningham, C. H. Hendon and V. J. Derose, *J. Am. Chem. Soc.*, 2019, **141**, 28.
- 13 C. E. Mcdevitt, M. V Yglesias, A. M. Mroz, E. C. Sutton, M. C. Yang, C. H. Hendon and V. J. Derose, *JBIC J. Biol. Inorg. Chem.*, 2019, **24**, 899–908.